



## Research paper

# Methylation and acetylation of 15-hydroxyanandamide modulate its interaction with the endocannabinoid system<sup>☆</sup>

Daniele Amadio<sup>a,1</sup>, Filomena Fezza<sup>a,b,1</sup>, Giuseppina Catanzaro<sup>b,c</sup>, Ottaviano Incani<sup>d</sup>, Guus van Zadelhoff<sup>e</sup>, Alessandro Finazzi Agrò<sup>a</sup>, Mauro Maccarrone<sup>b,c,\*</sup>

<sup>a</sup> Department of Experimental Medicine and Biochemical Sciences, University of Rome, Tor Vergata, Rome, Italy

<sup>b</sup> European Center for Brain Research (CERC)/Santa Lucia Foundation IRCCS, Rome, Italy

<sup>c</sup> Department of Biomedical Sciences, University of Teramo, Piazza A. Moro 45, 64100 Teramo, Italy

<sup>d</sup> Colosseum Combinatorial Chemistry, Centre for Technology, Rome, Italy

<sup>e</sup> Department of Chemistry, Utrecht University, Utrecht, The Netherlands

## ARTICLE INFO

## Article history:

Received 26 May 2009

Accepted 3 January 2010

Available online 21 January 2010

## Keywords:

Anandamide  
2-Arachidonoylglycerol  
Fatty acid amide hydrolase  
Natural inhibitors

## ABSTRACT

The biological activity of endocannabinoids like anandamide (AEA) and 2-arachidonoylglycerol (2-AG) is subjected *in vivo* to a “metabolic control”, exerted mainly by catabolic enzymes. AEA is inactivated by fatty acid amide hydrolase (FAAH), that is inhibited competitively by hydroxyanandamides (HAEAs) generated from AEA by lipoxygenase activity. Among these derivatives, 15-HAEA has been shown to be an effective ( $K_i \sim 0.6 \mu\text{M}$ ) FAAH inhibitor, that blocks also type-1 cannabinoid receptor (CB1R) but not other components of the “endocannabinoid system (ECS)”, like the AEA transporter (AMT) or CB2R. Here, we extended the study of the effect of 15-HAEA on the AEA synthetase (NAPE-PLD) and the AEA-binding vanilloid receptor (TRPV1), showing that 15-HAEA activates the former (up to  $\sim 140\%$  of controls) and inhibits the latter protein (down to  $\sim 70\%$ ). We also show that 15-HAEA halves the synthesis of 2-AG and almost doubles the transport of this compound across the membrane. In addition, we synthesized methyl and acetyl derivatives of 15-HAEA (15-MeOAEA and 15-AcOAEA, respectively), in order to check their ability to modulate FAAH and the other ECS elements. In fact, methylation and acetylation are common biochemical reactions in the cellular environment. We show that 15-MeOAEA, unlike 15-AcOAEA, is still a powerful competitive inhibitor of FAAH ( $K_i \sim 0.7 \mu\text{M}$ ), and that both derivatives have negligible interactions with the other proteins of ECS. Therefore, 15-MeOAEA is a FAAH inhibitor more selective than 15-HAEA. Further molecular dynamics analysis gave clues to the molecular requirements for the interaction of 15-HAEA and 15-MeOAEA with FAAH.

© 2010 Elsevier Masson SAS. All rights reserved.

**Abbreviations:** AEA, anandamide; 2-AG, 2-arachidonoylglycerol; FAAH, fatty acid amide hydrolase; HAEAs, hydroxyanandamides; ECS, endocannabinoid system; AMT, anandamide membrane transport; NAPE-PLD, *N*-acylphosphatidylethanolamine (NAPE)-hydrolyzing phospholipase D; MAGL, monoacylglycerol lipase; DAGL, diacylglycerol lipase; CB1R, type-1 cannabinoid receptors; CB2R, type-2 cannabinoid receptors; 15-HAEA, (15*S*)-hydroxy-(5*Z*,8*Z*,11*Z*,13*E*)eicosatetraenoyl-*N*-(2-hydroxyethyl)amine; 15-MeOAEA, (15*S*)-methoxy-(5*Z*,8*Z*,11*Z*,13*E*)eicosatetraenoyl-*N*-(2-hydroxyethyl)amine; 15-AcOAEA, (15*S*)-acetoxy-(5*Z*,8*Z*,11*Z*,13*E*)eicosatetraenoyl-*N*-(2-hydroxyethyl)amine; AA, arachidonic acid; 2-OG, 2-oleoylglycerol; RTX, resiniferatoxin; DAG, 1-Stearoyl-2-arachidonoyl-*sn*-glycerol; NArPE, *N*-arachidonoyl phosphatidylethanolamine; TBTU, *O*-(benzotriazol-1-yl)-*N,N,N',N'*-tetramethyluronium tetrafluoroborate; MAFP, methoxy arachidonoyl fluorophosphonate.

<sup>☆</sup> This investigation was partly supported by FILAS (FAAHI project 2006), and by Fondazione TERCAS (project 2009-2012).

\* Corresponding author at: Department of Biomedical Sciences, University of Teramo, Piazza A. Moro 45, 64100 Teramo, Italy. Tel.: +39 0861 266875; fax: +39 0861 266877.

E-mail address: [mmaccarrone@unite.it](mailto:mmaccarrone@unite.it) (M. Maccarrone).

<sup>1</sup> These authors equally contributed to this study.

## 1. Introduction

Anandamide (*N*-arachidonylethanolamine, AEA) and 2-arachidonoylglycerol (2-AG) are the most prominent members of a class of signaling molecules called “endocannabinoids” [1]. These substances are endogenous ligands of type-1 (CB1R) and type-2 (CB2R) cannabinoid receptors [2]. Additionally, AEA (but not 2-AG) can activate the transient receptor potential vanilloid 1 (TRPV1) [3].

AEA is mainly biosynthesized by a specific *N*-acylphosphatidylethanolamine (NAPE)-hydrolyzing phospholipase D (NAPE-PLD) [4], whereas the diacylglycerol lipase (DAGL) is the major enzyme responsible for the biosynthesis of 2-AG [5]. The biological actions of AEA and 2-AG are terminated by removal from the extracellular space, mediated by purported membrane transporters (AEA or 2-AG membrane transporters, AMT or 2-AGMT respectively) [6], followed by intracellular degradation by fatty acid amide hydrolase (FAAH) [7], or monoacylglycerol lipase (MAGL) [8]. Taken together,

receptors, metabolic enzymes and purported transporters of AEA, 2-AG and congeners form the “endocannabinoid system (ECS)” [9].

Among ECS components, only FAAH has been crystallized and found to be a homodimer of two 63 kDa subunits [7]. FAAH shows an unusual catalytic triad composed of serine-serine-lysine (Ser241-Ser217-Lys142), and has been demonstrated to be the key-regulator of endocannabinoid signaling *in vivo* [10]. On this basis, FAAH inhibitors hold the promise to become suitable therapeutic tools for several human diseases [11–14]. Although AEA is usually hydrolysed by FAAH, in blood cells like platelets and polymorphonuclear leukocytes it can alternatively be oxidized by lipoxygenase (LOX) [15,16]. AEA products generated by LOXs are known to play a role within the brain [16,17], and in general oxidized derivatives of AEA have a strong impact on cell functioning [18,19].

The main products generated from AEA by LOXs are hydroperoxyanandamides, which are quickly reduced to hydroxyanandamides (HAEAs) inside the cells [18]. All HAEAs competitively inhibit FAAH, with inhibition constant ( $K_i$ ) values in the  $\mu\text{M}$  range [20]. HAEAs also have a high degree of specificity towards other elements of the ECS, like AMT, CB1R or CB2R [20]. Remarkably, HAEAs are produced by the cell [21], and together with *N*-arachidonoylglycine [22] they represent the only natural FAAH inhibitors as yet known. Unlike most synthetic compounds, HAEAs are reversible inhibitor of enzyme activity, thus potentially allowing a more flexible modulation of the ECS *in vivo* [17].

Here, we sought to extend the study of the interaction of the most interesting HAEA, namely (15*S*)-hydroxy-(5*Z*,8*Z*,11*Z*,13*E*) eicosatetraenoyl-*N*-(2-hydroxyethyl)amine (15-HAEA), with NAPE-PLD and TRPV1, as well as with the proteins responsible for the synthesis (DAGL), transport (2-AGMT) and hydrolysis (MAGL) of 2-AG. As a matter of fact, 15-HAEA is the main product generated by 15-LOX from AEA, and is an effective ( $K_i \sim 0.6 \mu\text{M}$ ) natural inhibitor of FAAH [20]. Moreover, 15-HAEA might be subjected to two biochemical modifications, like methylation and acetylation, that represent reactions very common in the cell [23–25]. Our rationale was that methylation and acetylation of the hydroxyl group of HAEAs might modulate the interaction of these compounds with the ECS elements, and in particular with FAAH, in the cell. Therefore, in this study we developed synthetic routes in order to produce (15*S*)-methoxy-(5*Z*,8*Z*,11*Z*,13*E*)eicosatetraenoyl-*N*-(2-hydroxyethyl)amine (15-MeOAEA), and (15*S*)-acetoxy-(5*Z*,8*Z*,11*Z*,13*E*) eicosatetraenoyl-*N*-(2-hydroxyethyl)amine (15-AcOAEA). In addition, we modelled the interaction of AEA, 15-HAEA, 15-MeOAEA and 15-AcOAEA with the active site of FAAH, with the aim of clarifying some molecular details of the interaction of these compounds with the enzyme.

## 2. Materials and methods

### 2.1. Materials

Chemicals were of purest analytical grade, and all solvents were of HPLC grade. Arachidonic acid (AA), AEA, linoleic acid, 2-oleoylglycerol (2-OG), phosphatidylethanolamine (PE), CP55,940, resiniferatoxin (RTX) and 4-ethylmorpholine were from Sigma Chemical Co. (St. Louis, MO, USA). *N*-Arachidonoylphosphatidylethanolamine (NArPE) was synthesized from AA and PE as reported previously [26]. 1-Stearoyl-2-arachidonoyl-*sn*-glycerol (DAG) and 2-AG were from Alexis (Cornerstone, San Diego, USA). Esterase from porcine liver was purchased from Sigma Chemical Co. TBTU (*O*-(benzotriazol-1-yl)-*N,N,N'*-tetramethyluronium tetrafluoroborate) was from Novabiochem (Merck Biosciences AG, Switzerland). [ $^3\text{H}$ ]-AEA (179 Ci/mmol), [ $^3\text{H}$ ]-CP55,940 (126 Ci/mmol) and [ $^3\text{H}$ ]-RTX (43 Ci/mmol) were purchased from Perkin Elmer Life Science

(Boston, MA, USA). [ $^{14}\text{C}$ ]-DAG (56 mCi/mmol) was from Amersham (Little Chalfont, Bucks, UK). [ $^3\text{H}$ ]-NArPE (200 Ci/mmol) and [ $^3\text{H}$ ]-2-OG (20 Ci/mmol) were from ARC (St Louis, MO, USA).

### 2.2. Purification of soybean 15-LOX-1

15-LOX-1 was purified from soybean (*Glycine max* (L.) Merrill, Dolores) seeds (Saatbau Linz, Austria) on CM Sephadex C-50 and DEAE Sepharose columns (Pharmacia, Uppsala, Sweden), and was then subjected to a further step of purification by fast-protein liquid chromatography (FPLC, size-exclusion column Superdex-200) using an AKTA Explorer apparatus (Pharmacia), as described [27]. 15-LOX-1 (2  $\mu\text{M}$ ) activity was assayed spectrophotometrically at 25 °C in 0.1 M sodium borate buffer (pH = 9.0), by recording the formation of conjugated hydroperoxides from linoleic acid (40  $\mu\text{M}$ ) at 234 nm [27]. 15-LOX-1 was used to generate 15-HAEA, as described below, following a published procedure [28].

### 2.3. Synthesis of (15*S*)-hydroxy-5,8,11,13-eicosatetraenoic acid ((15*S*)-HETE)

10 U purified 15-LOX-1 were added to 100  $\mu\text{M}$  arachidonic acid (AA) in 250 ml of sodium borate buffer (0.1 M, pH = 9.0) at room temperature (r.t.). After 10 min the pH of the reaction was brought down to 4.5 with 1.0 M acetic acid and the reaction products were purified by SPE (OASIS HLB, 500 mg; Waters, Milford, MA, USA). The 15-HPETE was reduced with an excess of sodium borohydride at 0 °C under a gentle stream of nitrogen. After 30 min, the pH was lowered and the reaction product was purified with SPE (OASIS HLB, 100 mg). The AA derivatives were purified by reverse phase-high performance liquid chromatography (RP-HPLC), using an 1090 LC chromatographer equipped with a 1040A diode array detector (Hewlett–Packard, Palo Alto, CA, USA) and a cosmosil 5C18 ARII column (5  $\mu\text{m}$ , 250  $\times$  4.6 mm, Nacalai Tesque, Kyoto, Japan). Separations were performed at a flow rate of 1 ml/min with a 10 min linear gradient of methanol/water/acetic acid, from 75/25/0.1 to 95/5/0.1 (v/v/v), followed by 5 min at the latter conditions [28].

### 2.4. Synthesis of (15*S*)-methoxy-5,8,11,13-eicosatetraenoic acid ((15*S*)-MeOETE)

The purified 15-HETE was esterified with an excess of ethereal diazomethane at r.t. under nitrogen. After 30 min the excess of diazomethane was evaporated under a flow of nitrogen. The esterified AA derivative was dissolved in 100  $\mu\text{l}$  DMSO, cooled down to –20 °C, then 100  $\mu\text{l}$  methyl iodine was added. The reaction continued for 1 h, then the excess of methyl iodine was evaporated for 2 min under a gentle flow of nitrogen. The sample was purified by SPE and RP-HPLC, as described above. After purification of the methoxy-eicosatetraenoic acid methyl ester, the methyl ester of the carboxylic acid was removed with 200 U esterase (from porcine liver) in 100 ml sodium borate (10 mM, pH = 8.0) at r.t. After 1 h the sample was purified with SPE.

### 2.5. Synthesis of (15*S*)-acetoxy-5,8,11,13-eicosatetraenoic acid ((15*S*)-AcOETE)

The purified 15-HETE was esterified with an excess of ethereal diazomethane at r.t. under nitrogen. After 30 min the excess of diazomethane was evaporated under a nitrogen flow. The esterified AA derivative was dissolved in 500  $\mu\text{l}$  acetic anhydride/pyridine (1/1, v/v). The acetylation was completed after 30 min at 85 °C. After cooling down, 1 ml of methanol was added and after mixing, 9 ml of 50 mM acetic acid was added. The sample was purified by SPE and

RP-HPLC as described above. After purification of the acetoxy-eicosatetraenoic acid methyl ester, the methyl ester of the carboxylic acid was removed with 200 U esterase, in 100 ml sodium borate (10 mM, pH = 8.0) at r.t. After 1 h the sample was purified with SPE.

#### 2.6. Synthesis of methoxy- and acetoxy-eicosatetraenoylethanolamides (15-MeOAEA and 15-AcOAEA)

The synthetic routes for 15-MeOAEA and 15-AcOAEA are schematically depicted in Fig. 1. The purified AA derivatives were

dissolved in 250  $\mu$ l dimethylformamide and subsequently 0.95 eq. of TBTU (*O*-(benzotriazol-1-yl)-*N,N,N',N'*-tetramethyluronium tetrafluoroborate) and 1.5 eq. of 4-ethylmorpholine were added. After 5 min, 3 eq. of ethanolamine were added and the solution was allowed to react for 2 h at r.t. under nitrogen. Then, 1 ml of methanol and 9 ml of water were added to the reaction mixture, and the products were purified as described above.

The final products were both >95% pure by HPLC, and were reduced, hydrogenated, trimethyl silylated and analyzed by GC/MS as reported [28]. In particular, the GC/MS spectrum of 15-MeOAEA

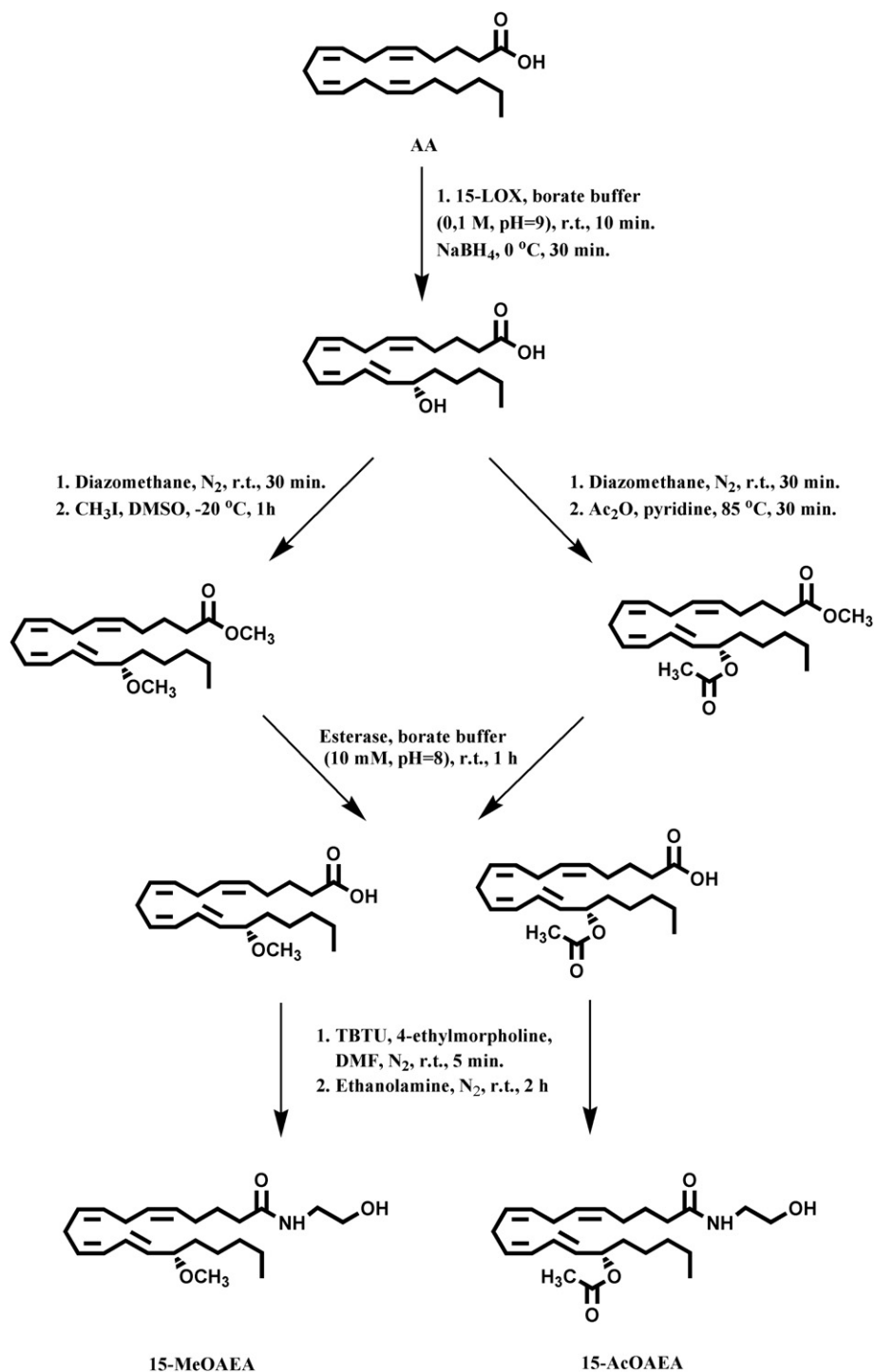


Fig. 1. Schematic representation of the synthetic routes for 15-MeOAEA and 15-AcOAEA (see Materials and methods for details).

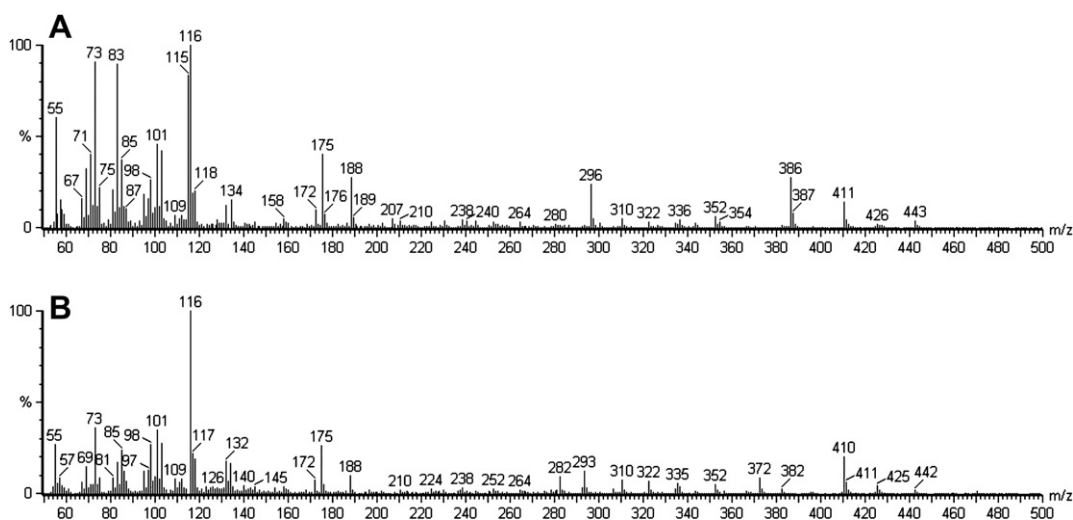


Fig. 2. GC/MS analysis of 15-MeOAEA (A) and 15-AcOAEA (B) (For experimental details see [Materials and methods](#)).

is shown in [Fig. 2A](#). Prominent fragments were:  $[M^+ - CH_3]$ ,  $m/z$  443 (5%);  $[CH_3 - O - CH - (CH_2)_{13} - CONH - (CH_2)_2 - OTMS^+]$ ,  $m/z$  386 (26%);  $[CH_3 - O - CH - (CH_2)_{13} - CONH - (CH_2)_2 - HOTMS^+]$ ,  $m/z$  296 (23%);  $[CH_3 - O - CH - (CH_2)_4 - CH_3^+]$ ,  $m/z$  115 (83%) and  $m/z$  116 (diagnostic ethanolamine fragment) (100%) [29,30]. Also 15-AcOAEA was characterized by GC/MS after derivatization with TMS ([Fig. 2B](#)). Characteristic fragmentations were:  $[M^+ - CH_3]$ ,  $m/z$  470 (1%);  $[M^+ - HOAc]$ ,  $m/z$  425 (3%);  $[M^+ - HOAc - CH_3]$ ,  $m/z$  410 (20%);  $[CH_3 - CO - O - CH - (CH_2)_{13} - CONH - (CH_2)_2 - OTMS^+ - C_2H_5O]$ ,  $m/z$  372 (9%);  $[M^+ - HOTMS - HOAc]$ ,  $m/z$  335 (5%);  $[M^+ - HOTMS - HOAc - C_2H_5O]$ ,  $m/z$  293 (12%);  $m/z$  116 (diagnostic ethanolamine fragment) (100%). The overall yields of the synthetic routes were ~30% for 15-MeOAEA and ~35% for 15-AcOAEA, starting from AA.

### 2.7. Assays of AEA metabolism

The synthesis of AEA through the activity of NAPE-PLD was assayed with murine brain homogenates (200  $\mu$ g/test), using 100  $\mu$ M  $[^3H]$ -NArPE as substrate [26]. The uptake of 500 nM  $[^3H]$ -AEA by AMT was measured with murine synaptosomes (100  $\mu$ g/test) as previously described [31]. The hydrolysis of 10  $\mu$ M  $[^3H]$ -AEA by FAAH was assayed with murine brain homogenates (40  $\mu$ g/test), by measuring the release of  $[^3H]$ -AA from  $[^3H]$ -AEA through RP-HPLC, as reported [32]. The effects of 15-HAEA, 15-MeOAEA and 15-AcOAEA on NAPE-PLD, AMT and FAAH activity were determined by adding each substance to the reaction mixture 15 min before the radiolabelled substrates. For kinetic studies of FAAH activity, different concentrations of  $[^3H]$ AEA (in the range of 0–30  $\mu$ M) and of inhibitor (0–5.0  $\mu$ M) were used, in order to determine apparent Michaelis–Menten constant ( $K_m$ ), maximum velocity ( $V_{max}$ ) and  $K_i$  by nonlinear regression analysis. To this aim, kinetic data were fitted to Michaelis–Menten curves, that were subjected to nonlinear regression analysis through the Prism4<sup>®</sup> program (GraphPAD Software for Science, San Diego, CA, USA). The same Michaelis–Menten curves were also analyzed by Lineweaver–Burk diagrams (double-reciprocal plots), in order to further visualize the type of inhibition.

### 2.8. Assays of 2-AG metabolism

The synthesis of 2-AG by DAGL was assayed with mouse brain homogenates (100  $\mu$ g protein/test), using 100  $\mu$ M  $[^{14}C]$ -DAG as

substrate [5]. The uptake of 500 nM  $[^3H]$ -2-AG by 2-AGMT was measured with murine synaptosomes (100  $\mu$ g/test), as described above for AMT. The hydrolysis of 2-AG by MAGL was measured with mouse brain supernatants (100  $\mu$ g protein/test), using 10  $\mu$ M  $[^3H]$ -2-OG as substrate [8]. The effects of 15-HAEA, 15-MeOAEA and 15-AcOAEA on DAGL, 2-AGMT and MAGL activity were tested by adding each compound to the reaction mixture 15 min before the radiolabelled substrates.

### 2.9. Binding to cannabinoid and vanilloid receptors

Membrane fractions isolated from mouse brain were used in rapid filtration assays with the synthetic cannabinoid  $[^3H]$ -CP55.940 (500 pM), in the presence of the protease inhibitor phenylmethylsulphonyl fluoride (50  $\mu$ M) as described [33]. The membrane fractions were used also to test the effect of the compounds on the binding of TRPV1 agonist  $[^3H]$ -RTX (500 pM) by rapid filtration assay [33]. In all experiments, unspecific binding was determined in the presence of an excess (1  $\mu$ M) of “cold” agonist (CP55.940 or RTX, respectively), as reported [33]. The effects of 15-HAEA, 15-MeOAEA and 15-AcOAEA on CB1R, CB2R and TRPV1 receptors were tested by adding each compound to the reaction mixture 15 min before the radiolabelled ligands.

### 2.10. Molecular modelling of FAAH

The crystal structure of FAAH (Protein Data Bank file 1MT5) [34], complexed with the irreversible inhibitor methoxy arachidonoyl fluorophosphonate (MAFP), was used as a reference to model the complexes of FAAH with AEA, 15-HAEA, 15-MeOAEA and 15-AcOAEA. The structure of the enzyme was prepared using the module Leap of the program AMBER [35] to add all the missing atoms to the system; the catalytic lysine was built as neutral. The structure was then imported in MOE [36] and energy-minimized, by using the Amber99 force field and the Born solvation model with dielectric constants of 4 and 80 for the interior and the exterior, respectively.

The optimization of the geometry was carried out in four steps: 1) Energy minimization with restraints (100 kcal mol<sup>-1</sup> Å<sup>-2</sup>) applied to heavy atoms; 2) minimization of the side-chains not present in the X-ray structure (missing atoms of the pdb); 3) energy minimization of the system with restraints (50 kcal mol<sup>-1</sup> Å<sup>-2</sup>)

applied to backbone atoms; 4) full minimization of the system. AEA was built using the geometry of MAFFP as a template. Molecular graphics techniques were used to modify the polar head of MAFFP (covalently bound to FAAH) and to convert it into AEA. To obtain a reasonable starting geometry of the FAAH/AEA complex, only few torsions were manually rotated, namely C3–C2, C2–C1, C1–N; the fatty acid chain of the molecule was kept fixed, while the polar head was rearranged in the cavity of the enzyme. The geometry of the FAAH/AEA complex was optimized in three steps: 1) energy minimization of AEA and all the atoms within 9 Å from any atom of the ligand with restraints on the backbone atoms; 2) restrained minimization of all the atoms of the system; 3) full minimization. The Amber99 force field with Born solvation was used. The structure of AEA was then used to build the analogues oxydated at C15 with few graphic manipulations of the substituent in the case of 15-AcOAEA, to eliminate overlapping with the surrounding enzyme atoms. The complexes were then energy-minimized as described for AEA. Visual inspection of modelled complexes and ligands was performed with PyMOL [37]. The analysis of enzyme channels was conducted with the CAVER [38], freely available as PyMOL plugin and as a stand-alone program.

### 2.11. Molecular dynamics

The four complexes of FAAH with AEA, 15-HAEA, 15-MeOAEA or 15-AcOAEA were subjected to 2 ns MD simulations, using MOE with Amber99 force field as described above. For each run, the fully-minimized structure was equilibrated for 0.5 ns with subsequent runs at 20, 100, 200, and 300 K. Then, a 1.5 ns MD run at 300 K was used to analyze the systems. For each modelled system, the MD trajectory was analyzed measuring several intra- and inter-molecular geometrical features. In particular, the geometry of the catalytic triad, the interaction with the nucleophile center of the ligand, and the interaction of the ligand with Met191 and Gly240 were monitored, in order to investigate the polar moiety of the ligand. The fatty acid moieties of the ligands were analyzed measuring the dihedral torsions of the fatty chain. The hydrophobic interaction with the enzyme cavity was also measured.

### 2.12. Statistical analysis

Data reported in this paper are the mean ( $\pm$ S.D.) of at least three independent determinations, each in duplicate. Statistical analysis was performed by nonparametric Mann–Whitney *U* test, elaborating experimental data by means of the GraphPad Prism4® (GraphPAD Software for Science, San Diego, CA, USA).

## 3. Results

### 3.1. Effects of 15-HAEA, 15-MeOAEA and 15-AcOAEA on AEA metabolism

We tested all compounds in the 0–1  $\mu$ M range, in order to ascertain their effects at physiologically relevant concentrations [20,21]. First of all, we found that 15-HAEA dose-dependently increased NAPE-PLD activity, with a maximum effect ( $\sim$ 140% of untreated controls) at 1  $\mu$ M. Instead, 15-MeOAEA or 15-AcOAEA were found to be ineffective under the same conditions (Table 1, and data not shown). On the other hand, 1  $\mu$ M 15-HAEA reduced AEA transport by AMT to  $\sim$ 70% of controls (Table 1), in keeping with previous data [20], and similarly to 1  $\mu$ M 15-MeOAEA ( $\sim$ 75%) but not to 1  $\mu$ M 15-AcOAEA that was ineffective (Table 1). The activity of FAAH was markedly reduced ( $\sim$ 30%) by 1  $\mu$ M 15-HAEA, as expected [20], and by 15-MeOAEA with a maximum effect ( $\sim$ 30%) at 1  $\mu$ M (Table 1). Instead, 15-AcOAEA had no significant effect under the same experimental conditions (Table 1). To further investigate the inhibition of FAAH by 15-MeOAEA, a more detailed kinetic analysis was performed. Nonlinear regression analysis of the kinetic data allowed to calculate the following apparent  $K_m$  ( $\mu$ M) and  $V_{max}$  (pmol/min per mg protein) values for [ $^3$ H]-AEA hydrolysis: controls =  $3.3 \pm 1.2$  and  $304 \pm 24$ ; 0.5  $\mu$ M 15-MeOAEA =  $6.3 \pm 2.1$  and  $297 \pm 31$ ; 5.0  $\mu$ M 15-MeOAEA =  $25.2 \pm 5.0$  and  $276 \pm 44$ . From these data, a  $K_i$  of  $0.68 \pm 0.14$   $\mu$ M was calculated, that is very close to that ( $K_i = 0.63 \pm 0.03$   $\mu$ M) already reported for FAAH inhibition by 15-HAEA [20]. The type of inhibition was competitive, because the difference between  $K_m$  of controls and that of 15-MeOAEA was statistically significant ( $p < 0.01$  at both inhibitor concentrations), whereas the difference between  $V_{max}$  values was not ( $p > 0.05$  in both cases). In addition, Lineweaver–Burk analysis of the same Michaelis–Menten curves further showed that the type of inhibition of 15-MeOAEA was competitive (Fig. 3B). Incidentally, both  $K_m$  and  $V_{max}$  values of [ $^3$ H]-AEA hydrolysis by FAAH were in keeping with previous reports [20,32].

### 3.2. Effects of 15-HAEA, 15-MeOAEA and 15-AcOAEA on 2-AG metabolism

Next, we studied the effect of AEA derivatives on the synthetic and hydrolytic enzymes responsible for 2-AG metabolism. We found that 15-HAEA exerts a dose-dependent inhibition of DAGL, with a maximum effect (50% of controls) at 1  $\mu$ M (Table 1, and data not shown). Instead, when we tested 15-MeOAEA and 15-AcOAEA in the same concentration range (0–1  $\mu$ M), no significant change of

**Table 1**  
Effect of 1  $\mu$ M 15-HAEA, 15-MeOAEA and 15-AcOAEA on the Elements of the Endocannabinoid System.

Compound	Control	15-HAEA	15-MeOAEA	15-AcOAEA
NAPE-PLD activity (pmol/min per mg protein)	14 $\pm$ 1 (100%)	19 $\pm$ 2* (136%)	12 $\pm$ 1# (86%)	14 $\pm$ 1# (100%)
AMT activity (pmol/min per mg protein)	0.80 $\pm$ 0.10 (100%)	0.57 $\pm$ 0.04* (72%)	0.62 $\pm$ 0.04* (77%)	0.77 $\pm$ 0.05# (96%)
FAAH activity (pmol/min per mg protein)	210 $\pm$ 15 (100%)	59 $\pm$ 4** (28%)	69 $\pm$ 3** (33%)	181 $\pm$ 11§ (86%)
DAGL activity (pmol/min per mg protein)	398 $\pm$ 14 (100%)	199 $\pm$ 12** (50%)	386 $\pm$ 15§ (97%)	339 $\pm$ 10§ (85%)
2-AGMT activity (pmol/min per mg protein)	2.0 $\pm$ 0.2 (100%)	3.6 $\pm$ 0.3** (180%)	2.2 $\pm$ 0.2§ (110%)	1.9 $\pm$ 0.2§ (95%)
MAGL activity (pmol/min per mg protein)	511 $\pm$ 41 (100%)	470 $\pm$ 38 (92%)	562 $\pm$ 56 (110%)	536 $\pm$ 38 (105%)
CB1R binding (fmol/mg protein)	112 $\pm$ 12 (100%)	32 $\pm$ 3** (28%)	83 $\pm$ 6*§ (74%)	86 $\pm$ 5*§ (77%)
CB2R binding (fmol/mg protein)	27 $\pm$ 3 (100%)	27 $\pm$ 2 (100%)	24 $\pm$ 2 (89%)	24 $\pm$ 2 (89%)
TRPV1 binding (fmol/mg protein)	220 $\pm$ 25 (100%)	165 $\pm$ 14* (75%)	221 $\pm$ 20# (100%)	213 $\pm$ 19# (97%)

\* $p < 0.05$  and \*\* $p < 0.01$  versus control; # $p < 0.05$  and § $p < 0.01$  versus 15-HAEA.

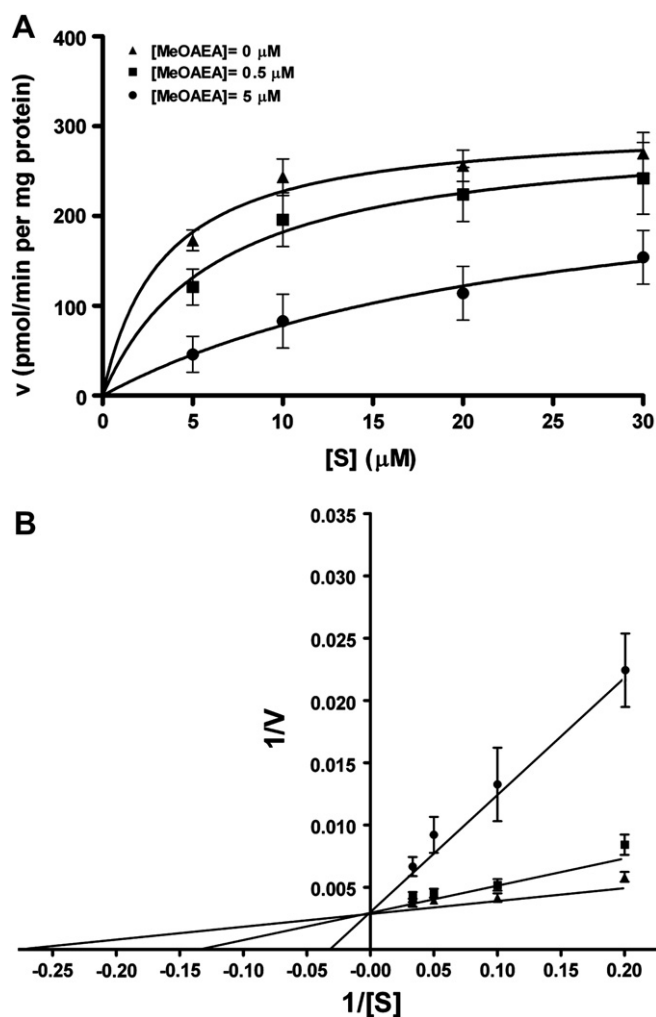


**Fig. 3.** Kinetic analysis of FAAH. (A) Michaelis–Menten curves of [ $^3\text{H}$ ]AEA hydrolysis by FAAH, determined by using different concentrations of substrate (0–30  $\mu\text{M}$  range) and of MeOAEA (0–5.0  $\mu\text{M}$  range). (B) Lineweaver–Burk analysis of the same Michaelis–Menten curves shown in panel A. It should be recalled that in double-reciprocal plots ( $1/v$  versus  $1/[S]$ ) the intercept on the y axis corresponds to  $1/V_{\text{max}}$ , whereas that on the x axis corresponds to  $-1/K_m$ .

DAGL activity could be observed (Table 1). Then, we investigated the effect of 15-HAEA and its derivatives on the transport of [ $^3\text{H}$ ]–2-AG by 2-AGMT. We found that 15-HAEA dose-dependently increases 2-AGMT activity, up to a maximum of  $\sim 180\%$  of the controls at 1  $\mu\text{M}$ , whereas 1  $\mu\text{M}$  15-MeOAEA or 1  $\mu\text{M}$  AcOAEA were ineffective (Table 1). Finally, we found that 15-HAEA did not exhibit any significant effect on the main 2-AG hydrolase, MAGL, when used at concentrations up to 1  $\mu\text{M}$ , and neither did 15-MeOAEA or 15-AcOAEA (Table 1).

### 3.3. Effects of 15-HAEA, 15-MeOAEA and 15-AcOAEA on cannabinoid and vanilloid receptors

To test the ability of 15-HAEA and its methyl and acetyl derivatives to affect CB1R and CB2R binding, competition binding assays were performed and the displacement of [ $^3\text{H}$ ]–CP55,940 was measured. As expected, 1  $\mu\text{M}$  15-HAEA reduced [ $^3\text{H}$ ]–CP55,940 binding to CB1R (down to  $\sim 30\%$  of controls) but not that to CB2R [20], whereas 15-MeOAEA and 15-AcOAEA were much less effective on CB1R binding ( $\sim 75\%$  of controls), and did not affect at all CB2R at concentrations up to 1  $\mu\text{M}$  (Table 1). In addition, we found that

15-HAEA reduced [ $^3\text{H}$ ]–RTX binding to TRPV1 receptors down to  $\sim 70\%$  of controls at 1  $\mu\text{M}$ , whereas 15-MeOAEA and 15-AcOAEA were ineffective under the same conditions (Table 1).

### 3.4. Molecular modelling and molecular dynamics analysis

In a final set of experiments we focused on the molecular requirements that might affect the interaction of FAAH with AEA and its derivatives. We show that AEA might enter the active site of FAAH directly from the plasma membrane (Fig. 4A) and, once cleaved off, the released polar amine can reach the cytosolic port through the internal channel present in the protein (Fig. 4A). The structural and dynamic features of AEA and its derivatives in the binding pocket of FAAH (Fig. 4B) were investigated by using molecular dynamics (MD) simulations. To highlight the bound conformations of the compounds, the MD trajectories were clustered using the program MOLINE [39]. Table 2 reports the results of the cluster analysis. The RMSD (Root Mean Square Deviation) in the spatial positions of the heavy atoms of the ligand was used to collect the representative conformers of the ligand in the pocket of the enzyme. A threshold of 0.5  $\text{\AA}$  in RMSD was used to distinguish structurally different conformers. To estimate the induced-fit from the enzyme on the conformation of the ligand, the bound conformations of the ligand were relaxed without the enzyme. Fig. 4C shows the representative conformers of AEA in the binding site of the enzyme, while Fig. 4D shows the conformers of 15-HAEA. The latter ligand had 5 bound conformers more than AEA. Moreover, the energy differences between bound conformers and the nearest free conformers is higher for AEA than for 15-HAEA. As shown in Table 2, the difference between the most stable conformation in the free and bound state is  $\sim 25 \text{ kcal mol}^{-1}$  for AEA and only 15  $\text{kcal mol}^{-1}$  for 15-HAEA. Moreover, the structures of AEA within the enzyme show a close similarity, while the conformations of 15-HAEA are more distinct, especially in the C16–C20 tail, because the hydroxyl group is well-oriented in the enzyme cavity. Fig. 4E and F report the hydrogen-bonding interactions observed from the molecular modelling analysis of 15-HAEA and 15-MeOAEA, whose structures were rendered using the PyMOL program [28]. From these models it can be calculated that FAAH/15-HAEA complex is favoured by three possible H-bonds (namely with Leu372, Glu373, and Ser376), while interaction of FAAH with 15-MeOAEA allows H-bond interactions with only one amino acid, Tyr335. Therefore, the presence of a methyl group seems to reduce the stability of the protein/ligand complex, although 15-MeOAEA can be still accommodated within the binding site of FAAH. Instead, 15-AcOAEA was found to be unable to generate hydrogen bonds with FAAH (data not shown), and hence it is not likely to be accommodated into the enzyme active site, due to the hindrance of the acetoxy group.

## 4. Discussion

In the present study we have extended a previous investigation on the effects of 15-HAEA, a natural inhibitor of FAAH [20], to all elements of the endocannabinoid system. In addition, we have checked the role of methylation and acetylation of 15-HAEA on its ability to interact with ECS proteins.

First of all, it should be mentioned that endocannabinoids are found at nM– $\mu\text{M}$  concentrations in cells, tissues and body fluids of mammals [40–42]. Thus, doses up to 1  $\mu\text{M}$  are used in several experimental paradigms, and their biological activities are considered of physiological relevance [12,20,21,43]. On the other hand, HAEAs are rather unstable and difficult to measure in biological samples [20,21]. Yet, lipoxygenase metabolism of AEA (that generates HAEAs) has been demonstrated in rat brain and blood cells [16,19], and a similar oxidative metabolism of 2-AG has been

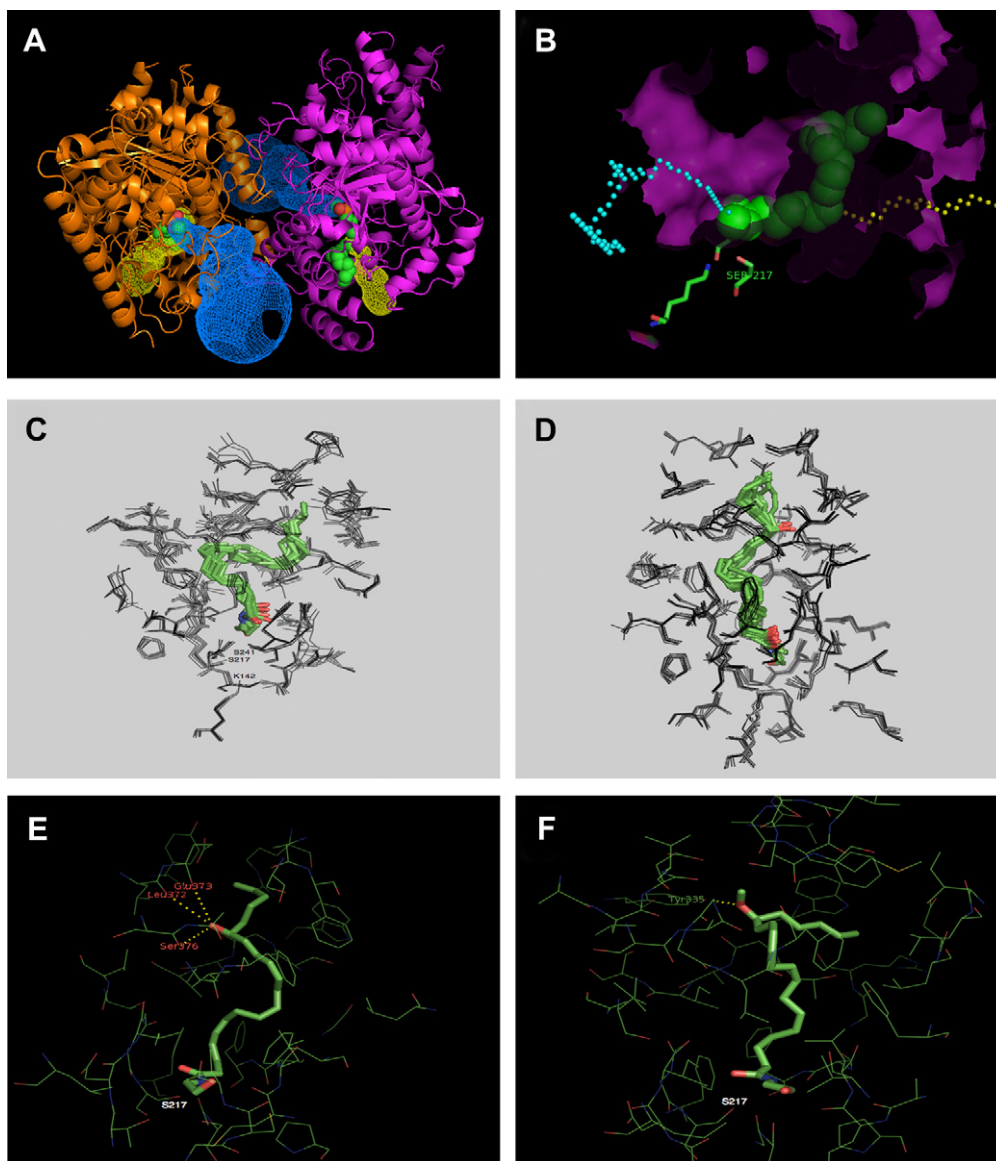


**Fig. 4.** Structure of FAAH and modelled complexes of FAAH with AEA and its analogues. (A) Static view of FAAH (cartoons of the two monomers in orange and magenta) cytosol (cyan) and membrane (yellow) ports computed with CAVER. The size of the channels indicates the available free volume for the entry of the substrate (solid sphere in CPK colours) and the exit of the products. (B) FAAH pocket (in magenta the solvent accessible molecular surface of FAAH), ligand (solid sphere in CPK colours), central paths through the channels to cytosol (yellow) and membrane (cyan). (C) Representative conformations of the MD trajectory for AEA. Ligand in solid stick (CPK colours). Residues within 5 Å from the ligand in grey. (D) Representative conformations of the MD trajectory for 15-HAEA. Ligand in solid stick (CPK colours). Residues within 5 Å from the ligand in grey. (E) H-bond interactions (yellow dashed lines) formed between the 15-hydroxyl group of 15-HAEA and Leu372, Glu373 and Ser376 of FAAH. (F) Only one H-bond is formed by 15-MeOAEA with the hydroxyl group of Tyr335 of FAAH.

shown in a eukaryotic cellular environment [18]. On this basis, we chose to investigate the effect of 15-HAEA and its derivatives in the 0–1  $\mu\text{M}$  range. In the same context, it should be stressed that the *in vivo* existence of 15-MeOAEA and 15-AcOAEA remains to be demonstrated, although these derivatives are likely to be formed by intact cells. In fact, methylation and acetylation are common post-translational protein modifications in the intracellular environment that can regulate protein activity, but they can also act as a modulatory mechanisms of bioactive compounds [23]. Interestingly, this is true for the regulation of the antibacterial properties of exogenous cannabinoids [44], and for the modulation of the activity of the endocannabinoid NADA [24]. It can be anticipated that, much alike HAEAs, more powerful analytical techniques need to be developed, in order to detect 15-MeOAEA and 15-AcOAEA in cells, tissues or biological fluids, thus confirming their physiological relevance.

We show that 15-HAEA, besides inhibiting AEA hydrolysis by FAAH, enhances AEA biosynthesis by NAPE-PLD, representing the first activator ever described for the latter enzyme. This finding might have therapeutic relevance for the treatment of human diseases where the activity of NAPE-PLD is decreased, and/or that of FAAH is increased [40]. In addition, 15-HAEA reduces 2-AG biosynthesis by DAGL and enhances 2-AG transport by 2-AGMT, overall reducing the extracellular content of this endocannabinoid. Therefore, 15-HAEA enhances the tone of AEA and reduces that of 2-AG, an opposite regulation that is in keeping with recent *in vivo* data, showing that one compound is up-regulated at the expenses of the other [13]. Incidentally, the observation that 2-AGMT is activated by 15-HAEA whereas AMT is inhibited is suggestive that the uptake of these two endocannabinoids across plasma membranes occurs via different transporters [45]. Finally, we show

**Table 2**

Cluster Analysis of AEA and 15-HAEA in the FAAH Pocket. (A) RMSD (Å) values between bound (upper triangle) and free conformers (lower triangle) of AEA in the pocket of FAAH. Bound conformers were derived from the clustering of MD trajectories in the pocket of FAAH using a threshold of 0.5 Å. Free conformers were obtained from the energy minimization of the ligand alone. (B) The same as AEA for 15-HAEA.

**A AEA**

		RMSD (Å)									Relative Energy (kcal/mol)			
		1	2*	3	4*	5	6	7	8	9	Bound	Free	Bound-Free	
<bound>		<b>1.3</b>	<b>1.3</b>	<b>1.2</b>	<b>1.2</b>	<b>1.4</b>	<b>1.3</b>	<b>1.4</b>	<b>1.3</b>	<b>1.5</b>				
1		-	0.7	0.8	0.9	1.4	1.6	1.7	1.6	1.8	17.0	4.5	12.5	
2		0.5	-	0.9	0.9	1.5	1.7	1.7	1.6	1.8	23.4	-	18.9	
3		1.0	1.0	-	0.2	1.3	1.4	1.6	1.5	1.7	14.0	6.5	7.4	
4		1.0	1.0	0.2	-	1.3	1.4	1.7	1.6	1.7	12.3	-	5.8	
5		2.4	2.4	2.3	2.3	-	1.0	1.5	1.5	1.6	24.9	2.9	22.0	
6		2.0	2.0	1.9	1.8	1.7	-	1.2	1.1	1.4	18.8	5.8	12.9	
7		3.2	3.2	3.3	3.3	2.7	2.7	-	0.9	1.3	15.1	2.8	12.4	
8		2.7	2.7	2.7	2.8	3.2	3.1	4.0	-	0.7	25.4	<b>0.0</b>	25.4	
9		3.2	3.2	3.1	3.1	3.4	3.5	4.5	2.2	-	9	12.9	0.8	12.1
<free>		<b>2.0</b>	<b>2.0</b>	<b>1.9</b>	<b>1.9</b>	<b>2.6</b>	<b>2.3</b>	<b>3.3</b>	<b>2.9</b>	<b>3.3</b>				

(\*) Bound conformers 2 and 4 collapses into free conformers 1 and 3 respectively. In bold, the mean average values.

**B 15-HAEA**

		RMSD (Å)														Relative Energy (kcal/mol)			
		1	2	3	4	5*	6	7	8	9	10*	11	12	13	14*	Bound	Free	Bound-Free	
<bound>		<b>1.5</b>	<b>1.5</b>	<b>1.3</b>	<b>1.3</b>	<b>1.3</b>	<b>1.3</b>	<b>1.2</b>	<b>1.2</b>	<b>1.3</b>	<b>1.2</b>	<b>1.3</b>	<b>1.3</b>	<b>1.3</b>	<b>1.4</b>				
1		-	0.8	0.9	1.3	1.0	1.5	1.6	1.8	1.7	1.7	1.6	1.9	1.8	2.0	17.5	1.7	15.8	
2		3.4	-	0.8	1.3	1.0	1.5	1.6	1.7	1.6	1.6	1.7	1.8	1.9	1.9	11.7	1.7	10.1	
3		3.7	1.0	-	1.0	0.4	1.2	1.3	1.5	1.5	1.5	1.5	1.8	1.7	1.7	11.3	1.8	9.6	
4		1.7	3.2	3.2	-	1.0	0.9	1.0	1.2	1.3	1.4	1.5	1.6	1.5	1.6	4	10.9	1.3	9.6
5		3.7	1.0	0.0	3.2	-	1.3	1.3	1.5	1.6	1.6	1.6	1.8	1.7	1.8	5	11.3	-	9.5
6		3.7	2.6	2.3	3.3	2.3	-	0.8	1.1	1.3	1.3	1.3	1.5	1.4	1.5	6	14.5	<b>0.0</b>	14.5
7		4.2	2.5	2.2	4.0	2.2	2.1	-	0.6	1.0	1.1	1.3	1.4	1.4	1.4	7	13.2	0.7	12.5
8		3.8	2.5	2.2	3.4	2.2	2.3	1.1	-	0.8	1.0	1.2	1.3	1.3	1.2	8	12.0	1.4	10.5
9		4.2	2.0	1.7	3.8	1.7	2.1	1.3	1.6	-	0.7	1.0	1.3	1.4	1.3	9	11.2	1.0	10.1
10		4.2	2.0	1.7	3.8	1.7	2.1	1.3	1.6	0.1	-	0.5	1.1	1.1	1.0	10	18.8	-	17.7
11		2.4	2.4	2.5	2.3	2.5	3.0	3.6	3.4	3.3	3.2	-	1.2	1.3	1.1	11	13.8	2.2	11.6
12		2.2	3.1	3.2	2.2	3.2	3.8	3.5	3.1	3.5	3.5	2.8	-	0.4	0.5	12	23.2	1.8	21.5
13		3.4	2.4	2.3	2.9	2.3	1.8	2.3	2.1	2.3	2.3	2.7	3.1	-	0.6	13	23.5	1.0	22.5
14		3.3	2.4	2.3	2.8	2.3	1.9	2.3	2.1	2.3	2.3	2.7	3.0	0.5	-	14	18.0	-	17.1
<free>		<b>3.4</b>	<b>2.3</b>	<b>2.2</b>	<b>3.1</b>	<b>2.2</b>	<b>2.6</b>	<b>2.5</b>	<b>2.4</b>	<b>2.3</b>	<b>2.3</b>	<b>2.8</b>	<b>3.1</b>	<b>2.3</b>	<b>2.3</b>				

(\*) Bound conformers 5, 10 and 14 collapse in free conformers 3, 9, and 13 respectively. In bold, the mean average values.

that 15-HAEA is also able to reduce RTX binding to TRPV1, although to a lower extent (~70% versus ~30% of controls) compared to its ability to reduce CB1R binding [20]. This finding suggests that hydroxylation of AEA might counteract neuroinflammatory pathologies, where both receptors are activated by an enhanced AEA tone [40]. On a general note, it should be stressed that our dose-dependence experiments can only identify the most effective dose within a purported physiological range (*i.e.*, up to 1  $\mu$ M), although they do not give information about the type of interaction between 15-HAEA derivatives and the various ECS targets. For instance, they do not clarify whether these compounds act as agonists, antagonists, inverse agonists or allosteric modulators of receptors, or as substrates for metabolic enzymes, an issue that could be clarified only by using radiolabelled compounds. However, the goal of defining the fine interaction of 15-HAEA derivatives with ECS elements goes far beyond the purposes of this investigation, and might be the subject of an independent study.

It is also noteworthy that 15-AcOAEA does not interact with any of the proteins that constitute the ECS, demonstrating that acetylation is sufficient to prevent interaction of 15-HAEA with all its targets within the ECS. Instead, methylation of 15-HAEA slightly

reduces its ability to inhibit FAAH ( $K_i$  values of ~0.7  $\mu$ M versus ~0.6  $\mu$ M), but improves its selectivity towards other ECS elements. In fact, 15-MeOAEA has no significant effect on NAPE-PLD, DAGL, 2-AGMT, or TRPV1, and shows less than half of the 15-HAEA effect on CB1R (1). Overall, 15-MeOAEA seems to be a better (more selective) inhibitor of FAAH than 15-HAEA. Incidentally, it can be noted that also the effect of 15-HAEA and 15-MeOAEA on AMT might simply be due to the inhibition of FAAH, that reduces the concentration gradient across the plasma membrane responsible for AEA uptake [46]. In this context, it seems noteworthy that methylation of the “endovanilloid” *N*-arachidonoyldopamine (NADA) by catechol-*O*-methyltransferase has been shown to lead to a methyl derivative (3-*O*-methyl-NADA) significantly less potent than NADA at TRPV1 [24], suggesting that methylation might represent a mechanism of partial inactivation of NADA within the brain, where methyltransferase activity is abundant [24]. These observations lend support to methylation of endocannabinoids as a biologically relevant process for the modulation of endocannabinoid signaling.

Molecular modelling of the internal channels of FAAH highlighted two possible ports which allow substrate entry from one side and product exit from another side, favoring the concept that

FAAH might operate via recruitment and release steps [7]. These ports are depicted in Fig. 4A and B. MD analysis of the interaction of 15-HAEA, 15-MeOAEA and 15-AcOAEA with FAAH demonstrated a larger flexibility of both ligands (Fig. 4C and D), suggestive of an entropic contribution that stabilizes their complexes with the enzyme, and hence their inhibitory properties. Furthermore, our simulations indicated that both enthalpic (larger H-bond network) and entropic factors (larger ligand flexibility) may favour the complexes of 15-HAEA and 15-MeOAEA with FAAH, compared to the complex with AEA (Fig. 4E and F), thus supporting the functional data on FAAH inhibition by these compounds (ref. 20 and this study). Instead, 15-AcOAEA cannot form hydrogen bonds with FAAH, nor can be accommodated in the binding pocket of the enzyme due to steric hindrance of the acetoxy group, thus explaining the lack of inhibitory properties. More in general, the constraints introduced by the hindrance of the acetyl group could account for the lack of interaction of 15-AcOAEA with the other ECS proteins, although MD simulations should be extended to the binding sites of these proteins to make more conclusive statements. In conclusion, we confirmed that endogenous products like hydroxanandamides can serve as physiological modulators of AEA effects on the proteins of the endocannabinoid system. In particular, we show that 15-HAEA inhibits FAAH and DAGL, while activating NAPE-PLD and 2-AGMT, overall increasing the tone and signaling of AEA, and reducing that of 2-AG. Therefore, 15-HAEA might be instrumental for the “yin–yang” regulation of AEA and 2-AG activity that has been observed in several physiological situations, both centrally and peripherally [13]. In addition, we investigated the effect of two potential endogenous derivatives of 15-HAEA, and show that methylation might be an easy way for the cell to transform 15-HAEA in a more selective FAAH inhibitor, with low affinity (if any) towards any other elements of the endocannabinoid system. Overall, it can be proposed that cells may know how to modulate endocannabinoid signaling through molecules much simpler than those synthesized in our laboratories to target the proteins of the ECS.

## References

- [1] V. Di Marzo, Endocannabinoids: synthesis and degradation. *Rev. Physiol. Biochem. Pharmacol.* 160 (2008) 1–24.
- [2] A.C. Howlett, F. Barth, T.I. Bonner, et al., International Union of Pharmacology. XXVII. Classification of cannabinoid receptors. *Pharmacol. Rev.* 54 (2002) 161–202.
- [3] K. Starowicz, L. Cristino, V. Di Marzo, TRPV1 receptors in the central nervous system: potential for previously unforeseen therapeutic applications. *Curr. Pharm. Des.* 14 (2008) 42–54.
- [4] Y. Okamoto, J. Morishita, K. Tsuboi, T. Tonai, N. Ueda, Molecular characterization of a phospholipase D generating anandamide and its congeners. *J. Biol. Chem.* 279 (2004) 5298–5305.
- [5] T. Bisogno, F. Howell, G. Williams, et al., Cloning of the first sn1-DAG lipases points to the spatial and temporal regulation of endocannabinoid signaling in the brain. *J. Cell Biol.* 163 (2003) 463–468.
- [6] A. Hermann, M. Kaczocha, D.G. Deutsch, 2-Arachidonoylglycerol (2-AG) membrane transport: history and outlook. *AAPS J.* 8 (2006) E409–E412.
- [7] M.K. McKinney, B.F. Cravatt, Structure and function of fatty acid amide hydrolase. *Annu. Rev. Biochem.* 74 (2005) 411–432.
- [8] T.P. Dinh, T.F. Freund, D. Piomelli, A role for monoglyceride lipase in 2-arachidonoylglycerol inactivation. *Chem. Phys. Lipids* 121 (2002) 149–158.
- [9] L. De Petrocellis, M.G. Cascio, V. Di Marzo, The endocannabinoid system: a general view and latest additions. *Br. J. Pharmacol.* 141 (2004) 765–774.
- [10] B.F. Cravatt, A.H. Lichtman, Fatty acid amide hydrolase: an emerging therapeutic target in the endocannabinoid system. *Curr. Opin. Chem. Biol.* 7 (2003) 469–475.
- [11] M. Maccarrone, Fatty acid amide hydrolase: a potential target for next generation therapeutics. *Curr. Pharm. Des.* 12 (2006) 759–772.
- [12] V. Di Marzo, Targeting the endocannabinoid system: to enhance or reduce? *Nat. Rev. Drug Discov.* 7 (2008) 438–455.
- [13] V. Di Marzo, M. Maccarrone, FAAH and anandamide: is 2-AG really the odd one out? *Trends Pharmacol. Sci.* 29 (2008) 229–233.
- [14] M. Seierstad, J.G. Breitenbucher, Discovery and development of fatty acid amide hydrolase (FAAH) inhibitors. *J. Med. Chem.* 51 (2008) 7327–7343.
- [15] W.S. Edgmond, C.J. Hillard, J.R. Falck, C.S. Kearn, W.B. Campbell, Human platelets and polymorphonuclear leukocytes synthesize oxygenated derivatives of arachidonylethanolamide (anandamide): their affinities for cannabinoid receptors and pathways of inactivation. *Mol. Pharmacol.* 54 (1998) 180–188.
- [16] W.B. Veldhuis, M. van der Stelt, M.W. Wadman, et al., Neuroprotection by the endogenous cannabinoid anandamide and arvanil against *in vivo* excitotoxicity in the rat: role of vanilloid receptors and lipoxygenases. *J. Neurosci.* 23 (2003) 4127–4133.
- [17] E. Dainese, V. Gasperi, M. Maccarrone, Partial QSAR analysis of some selected natural inhibitors of FAAH suggests a working hypothesis for the development of endocannabinoid-based drugs. *Curr. Drug Targets CNS Neurol. Disord.* 4 (2005) 709–714.
- [18] K.R. Kozak, L.J. Marnett, Oxidative metabolism of endocannabinoids. *Prostaglandins Leukot. Essent. Fatty Acids* 66 (2002) 211–220.
- [19] C.A. Rouzer, L.J. Marnett, Non-redundant functions of cyclooxygenases: oxygenation of endocannabinoids. *J. Biol. Chem.* 283 (2008) 8065–8069.
- [20] M. van der Stelt, J.A. van Kuik, M. Bari, et al., Oxygenated metabolites of anandamide and 2-arachidonoylglycerol: conformational analysis and interaction with cannabinoid receptors, membrane transporter, and fatty acid amide hydrolase. *J. Med. Chem.* 45 (2002) 3709–3720.
- [21] M. Maccarrone, Inhibition of anandamide hydrolysis: cells also know how to do it. *Trends Mol. Med.* 10 (2004) 13–14.
- [22] M.G. Cascio, A. Minassi, A. Ligresti, G. Appendino, S. Burstein, V. Di Marzo, A structure–activity relationship study on N-arachidonoyl-amino acids as possible endogenous inhibitors of fatty acid amide hydrolase. *Biochem. Biophys. Res. Commun.* 314 (2004) 192–196.
- [23] T.R. Cimato, J. Tang, Y. Xu, C. Guarnaccia, et al., Nerve growth factor-mediated increases in protein methylation occur predominantly at type I arginine methylation sites and involve protein arginine methyltransferase 1. *J. Neurosci. Res.* 67 (2002) 435–442.
- [24] S.M. Huang, T. Bisogno, M. Trevisani, et al., An endogenous capsaicin-like substance with high potency at recombinant and native vanilloid VR1 receptors. *Proc. Natl. Acad. Sci. U. S. A.* 99 (2002) 8400–8405.
- [25] M.P. Mattson, Methylation and acetylation in nervous system development and neurodegenerative disorders. *Ageing Res. Rev.* 2 (2003) 329–342.
- [26] F. Fezza, V. Gasperi, C. Mazzei, M. Maccarrone, Radiochromatographic assay of N-acyl-phosphatidylethanolamine-specific phospholipase D activity. *Anal. Biochem.* 339 (2005) 113–120.
- [27] E. Dainese, A. Sabatucci, G. Van Zadelhoff, et al., Structural stability of soybean lipoxygenase-1 in solution as probed by small angle X-ray scattering. *J. Mol. Biol.* 349 (2005) 143–152.
- [28] G. Van Zadelhoff, G.A. Veldink, J.F. Vlieghe, et al., With anandamide as substrate plant 5-lipoxygenases behave like 11-lipoxygenases. *Biochem. Biophys. Res. Commun.* 248 (1998) 33–38.
- [29] R. Shrestha, M.A. Noordermeer, M. van der Stelt, G.A. Veldink, K.D. Chapman, N-acyl-ethanolamines are metabolized by lipoxygenase and amidohydrolase in competing pathways during cottonseed imbibition. *Plant Physiol.* 130 (2002) 391–401.
- [30] L. Seipold, G. Gerlach, L. Wessjohann, A new type of floral oil from *Malpighia coccigera* (Malpighiaceae) and chemical considerations on the evolution of oil flowers. *Chem. Biodivers.* 1 (2004) 1519–1528.
- [31] F. Fezza, N. Battista, M. Bari, M. Maccarrone, Methods to assay anandamide hydrolysis and transport in synaptosomes. *Methods Mol. Med.* 123 (2006) 163–168.
- [32] M. Maccarrone, M. Bari, A. Finazzi-Agrò, A sensitive and specific radiochromatographic assay of fatty acid amide hydrolase activity. *Anal. Biochem.* 267 (1999) 314–318.
- [33] M. Maccarrone, B. Barboni, A. Paradisi, et al., Characterization of the endocannabinoid system in boar spermatozoa and implications for sperm capacitation and acrosome reaction. *J. Cell Sci.* 118 (2005) 4393–4404.
- [34] M.H. Bracey, M.A. Hanson, K.R. Masuda, R.C. Stevens, B.F. Cravatt, Structural adaptations in a membrane enzyme that terminates endocannabinoid signaling. *Science* 298 (2002) 1793–1796.
- [35] D.A. Case, T.A. Darden, T.E. Cheatham III, et al., AMBER 10. University of California, San Francisco, USA, 2008.
- [36] Molecular Operating Environment. Chemical Computing Group, Inc., Montreal, Quebec, 2008.
- [37] W.L. DeLano, The PyMOL Molecular Graphics System. DeLano Scientific LLC, Palo Alto, CA, USA, 2008.
- [38] M. Petrek, M. Otyepka, P. Banáš, P. Košíková, J. Koča, J. Damborský, Caver: a new tool to explore routes from protein clefts, pockets and cavities. *BMC Bioinformatics* 7 (2006) 316.
- [39] S. Alcaro, F. Gasparrini, O. Incani, L. Caglioti, M. Pierini, C. Villani, Quasi flexible automatic docking processing for studying stereoselective recognition mechanisms, part 2: prediction of  $\Delta G$  of complexation and  $^1\text{H}$  NMR NOE correlation. *J. Comput. Chem.* 28 (2007) 1119–1128.
- [40] D. Centonze, L. Battistini, M. Maccarrone, The endocannabinoid system in peripheral lymphocytes as a mirror of neuroinflammatory diseases. *Curr. Pharm. Des.* 14 (2008) 2370–2382.
- [41] M.G. Balvers, K.C. Verhoeckx, R.F. Witkamp, Development and validation of a quantitative method for the determination of 12 endocannabinoids and related compounds in human plasma using liquid chromatography–tandem mass spectrometry. *J. Chromatogr. B Analyt. Technol. Biomed. Life Sci.* 877 (2009) 1583–1590.
- [42] J. Palandra, J. Prusakiewicz, J.S. Ozer, Y. Zhang, T.G. Heath, Endogenous ethanolamide analysis in human plasma using HPLC tandem MS with

- electrospray ionization. *J. Chromatogr. B Analyt. Technol. Biomed. Life Sci.* 877 (2009) 2052–2060.
- [43] M. Maccarrone, S. Rossi, M. Bari, et al., Anandamide inhibits metabolism and physiological actions of 2-arachidonoylglycerol in the striatum. *Nat. Neurosci.* 11 (2008) 152–159.
- [44] G. Appendino, S. Gibbons, A. Giana, et al., Antibacterial cannabinoids from *Cannabis sativa*: a structure–activity study. *J. Nat. Prod.* 71 (2008) 1427–1430.
- [45] M.V. Catani, F. Fezza, S. Baldassarri, et al., Expression of the endocannabinoid system in the bi-potential HEL cell line: commitment to the megakaryoblastic lineage by 2-arachidonoylglycerol. *J. Mol. Med.* 87 (2009) 65–74.
- [46] D.G. Deutsch, S.T. Glaser, J.M. Howell, et al., The cellular uptake of anandamide is coupled to its breakdown by fatty-acid amide hydrolase. *J. Biol. Chem.* 276 (2001) 6967–6973.